American Journal of Pathology, Vol. 160, No. 5, May 2002
Copyright © American Society for Investigative Pathology

The Lysosomal Protease Cathepsin L Is an Important Regulator of Keratinocyte and Melanocyte Differentiation During Hair Follicle Morphogenesis and Cycling

Desmond J. Tobin,* Kerstin Foitzik,† Thomas Reinheckel,‡ Lars Mecklenburg,† Vladimir A. Botchkarev,§ Christoph Peters,‡ and Ralf Paus†

From the Department of Biomedical Sciences, University of Bradford, Bradford, England; the Department of Dermatology,† University Hospital Hamburg-Eppendorf, University of Hamburg, Hamburg, Germany; the Institute of Molecular Medicine,‡ University of Freiburg, Freiburg, Germany; and the Department of Dermatology,§ Boston University School of Medicine, Boston, Massachusetts*

We have previously shown that the ubiquitously expressed lysosomal cysteine protease, cathepsin L (CTSL), is essential for skin and hair follicle homeostasis. Here we examine the effect of CTSL deficiency on hair follicle development and cycling in *ctsl*$^{-/-}$ mice by light and electron microscopy, Ki67/terminal dUTP nick-end labeling, and trichohyalin immunofluorescence. Hair follicle morphogenesis in *ctsl*$^{-/-}$ mice was associated with several abnormalities. Defective terminal differentiation of keratinocytes occurred during the formation of the hair canal, resulting in disruption of hair shaft outgrowth. Both proliferation and apoptosis levels in keratinocytes and melanocytes were higher in *ctsl*$^{-/-}$ than in *ctsl*$^{+/+}$ hair follicles. The development of the hair follicle pigmentary unit was disrupted by vacuolation of differentiating melanocytes. Hair cycling was also abnormal in *ctsl*$^{-/-}$ mice. Final stages of hair follicle morphogenesis and the induction of hair follicle cycling were retarded. Thereafter, these follicles exhibited a truncated resting phase (telogen) and a premature entry into the first growth phase. Further abnormalities of telogen development included the defective anchoring of club hairs in the skin, which resulted in their abnormal shedding. Melanocyte vacuolation was again apparent during the hair cycle-associated reconstruction of the hair pigmentary unit. A hallmark of these *ctsl*$^{-/-}$ mice was the severe disruption in the exiting of hair shafts to the skin surface. This was mostly because of a failure of the inner root sheath (keratinocyte layer next to the hair shaft) to fully desquamate. These changes resulted in a massive dilation of the hair canal and the abnormal routing of sebaceous gland products to the skin surface. In summary, this study suggests novel roles for cathepsin proteases in skin, hair, and pigment biology. Principal target tissues that may contain protein substrate(s) for this cysteine protease include the developing hair cone, inner root sheath, anchoring apparatus of the telogen club, and organelles of lysosomal origin (eg, melanosomes). *(Am J Pathol 2002, 160:1807–1821)*

The hair follicle (HF) is a unique neuroectodermal-mesodermal interactive organoid that results in the elaboration of at least 15 distinct interacting cell subpopulations, organized into five or six concentric cylinders.[1–3] These together provide a truly exceptional miniorgan that rivals the vertebrate limb bud,[4] and feather and tooth development[5] as models for studies of the genetic regulation of morphogenesis and tissue renewal.[2,6,7] From its initiation during the perinatal period to its life-long cyclical growth, the HF is unique in the adult mammalian body in experiencing multiple and life-long recapitulations to early stages of its embryogenesis.[2,8] Critical to the formation of a functional hair fiber and the maintenance of the HF's cyclical behavior is the highly regulated expression of molecular mediators that form the HF. Although most investigations have focused on the role of classical morphogens, growth factors, and cytokines in the control of HF development and cycling,[3] recent evidence has also implicated an important role for protease/anti-protease systems. For example, there are distinct hair cycle-dependent changes in metalloproteases and their inhibitor systems.[9,10] Also, hepatocyte growth factor stimulates HF elongation in organ culture after activation by the serine proteinase, hepatocyte growth factor activator. This elongation can be partially abrogated by the serine

Supported in part by grants from the Deutsche Forschungsgemeinschaft [Pa 345/8-3 (to R. P. and K. F.) and Re 1584/1-2 (to T. R. and C. P.)] and from Procter & Gamble Ltd., UK (to D. J. T.).

Accepted for publication February 18, 2002.

Address reprint requests to Prof. Ralf Paus, Department of Dermatology, University Hospital Eppendorf, University of Hamburg, Martinistr 52, D-20246 Hamburg, Germany. E-mail: paus@uke.uni-hamburg.de.

proteinase inhibitor, aprotinin.[11,12] It has also been proposed that among other proteinases/protease inhibitors, gelatinase A,[13] nexin-1,[14] and stratum corneum chymotryptic enzyme[15] have a role in the regulation of hair growth and/or cycling.

In this context, the papain-like lysosomal cysteine protease, cathepsin L (CTSL), one of the major lysosomal enzymes that can also be secreted, is of particular interest. CTSL-deficient mice (*ctsl*$^{-/-}$) exhibit specific perturbations in both HF morphogenesis and cycling.[16,17] These, as yet ill-characterized abnormalities, deserve further dissection because they promise novel insights into the full range of functions of CTSL. This multifunctional, ubiquitously expressed, proteinase is involved in the positive thymic selection of CD4$^+$ T cells and the intrathymic degradation of the MHC class II invariant chain.[16] Recent reports also indicate a role for CTSL in bone resorption,[18] trophoblast invasion,[19,20] tumor metastasis,[21] and chronic inflammation.[22] *In vivo*, the level of CTSL mRNA is related to tumor progression/metastatic potential,[23] and this is thought to relate to the ability of CTSL to degrade extracellular matrix and basement membranes.[24] As part of its extracellular proteolytic activity, CTSL can hydrolyze azocasein, elastin, and collagen.[18,25] Expression of procathepsin L has been reported in normal epidermis, eccrine sweat glands, HFs, and blood vessels.[26]

Unlike other members of the mammalian papain family of cysteine proteases, the CTSL gene is activated by various growth factors[27,28] and oncogenes.[29] Many of these are also intimately involved in the regulation of hair growth. Notably, the pro-inflammatory cytokine interleukin-6 can up-regulate CTSL, whereas transforming growth factor-β1 suppresses CTSL expression.[30] Mice expressing the K14-interleukin-6 transgene exhibit retarded hair growth[31] while HF regression (catagen) is regulated in part by transforming growth factor-β1.[32] The level of CTSL mRNA in certain cell types is significantly increased by basic fibroblast growth factor and nerve growth factor.[33] Notably, basic fibroblast growth factor is a hair growth inhibitor in mice,[34] whereas nerve growth factor promotes murine HF development and the prohormone-responsive neuronal system has been implicated in the regulation of hair growth.[35] CTSL protease activity is also increased by interleukin-1β, interleukin-6, and oncostatin M, and decreased by insulin-like growth factor-1 and growth hormone,[36] ie, bioregulators appreciated as hair growth modulatory agents.[3,7,37] Furthermore, ras oncogenes (K-ras and N-ras) up-regulate CTSL activities to increase tumorigenic potential,[38] whereas mice overexpressing the *ras* activator, E2F1, exhibit HF development disrupted via increased apoptosis.[39]

Of related interest is the observation that CTSL can generate the angiogenesis inhibitor endostatin, pointing to a CTSL involvement in a regulatory loop of angiogenesis.[40] This is of trichological importance, because angiogenesis is fundamental to the HF switch from resting (telogen) to the active growth stage (anagen),[41] whereas HF regression (catagen) is associated with vascular regression.[42] In summary, there are numerous biological reasons why lack of functional CTSL may be expected to effect the HF.

Indeed, CTSL knockout mice exhibit significant alterations in skin homeostasis and striking defects in hair growth abnormalities. The epidermis of *ctsl*$^{-/-}$ mice is significantly thicker than that of *ctsl*$^{+/+}$ mice, because of increased epidermal proliferation.[17] Furless (*fs*) mice exhibit a very similar phenotype to *ctsl*$^{-/-}$ mice, because of allelism for *fs* and *ctsl* with a missense mutation (glycine to arginine substitution, G149R) which results in the loss of CTSL catalytic activity.[17]

HF morphogenesis and the initiation of the first HF regression phase (catagen), which sets off HF cycling,[3,8] are significantly delayed in *ctsl*$^{-/-}$ mice. However, null mice subsequently exhibit a much accelerated growth phase of the first genuine hair cycle (anagen).[17] Despite this accelerated entry into anagen, *ctsl*$^{-/-}$ mice are by then macroscopically nude, having shed all their fur during an apparently truncated and abnormal preceding catagen/telogen phase. After hair regrowth during each subsequent anagen phase, it falls out again with entry into catagen. Normally, the club hairs of telogen HFs in mice are not shed, instead being retained in the HF for several cycles until the hair shafts are shed in a separately controlled hair cycle phase (exogen).[3] However, hair loss and hair regrowth in later *ctsl*$^{-/-}$ hair cycles is both incomplete and spatially restricted, so that these mice always remain partially devoid of hair. The shedding of hair shafts has been ascribed to an abnormal formation of the telogen club.[17] This structure aids the persistent mooring of the hair shaft to its HF.[3,43] Interestingly, regrowing hair shafts become progressively grayer in *ctsl*$^{-/-}$ mice.[17]

The current morphological and cytokinetic study was conducted to examine more closely the nature of the defects underlying this intriguing phenotype using light microscopic and ultrastructural techniques. This should facilitate dissecting the functional roles of CTSL in HF biology in particular and epithelial and pigment cell biology in general. The specific questions addressed by this study were how CTSL deficiency affects postnatal HF development and cycling and what components of the developing and cycling HF are primarily targeted. Given that increased epidermal proliferation is a feature of this knockout,[17] the current study investigated proliferation, apoptosis, and terminal differentiation during HF development and cycling. Such events are critically dependent on spatiotemporally, stringently restricted cell proliferation and death.[3,44,45] We examined the involvement of CTSL in HF cycling from the first regression phase (catagen), formation of the telogen resting HF, hair shaft shedding or exogen,[37] and the subsequent HF regeneration during anagen. The possible involvement of the inner root sheath (IRS) structural protein, trichohyalin, a potential substrate for CTSL, was assessed immunohistochemically by protein expression in *ctsl*$^{-/-}$ and *ctsl*$^{+/+}$ HFs. Finally, the morphological basis for the observed canities (ie, hair graying) in *ctsl*$^{-/-}$ mice[17] was examined, as lysosome function (including their biogenic derivatives such as melanosomes,[46]) is likely to be affected by the absence of this lysosomal enzyme.

Materials and Methods

Animals and Tissues

Mice lacking CTSL expression (*ctsl*$^{-/-}$) were generated by insertion of a G418 resistance cassette in exon 3 of CTSL by homologous recombination in embryonic stem cells.[16,17] Expression of CTSL mRNA, protein, or CTSL activity was completely abolished in *ctsl*$^{-/-}$ mice.[17] The mice were housed in a controlled environment with a temperature of 21 ± 1°C and a 12-hour day/night cycle. Mice were kept in macrolon cages and had access to standard food pellets and tap water *ad libitum*. The microbiological status of the animal facility was checked according to our institutional guidelines. Mice were essentially pathogen-free. Most notably, ectoparasites and dermatophytes were not detectable. For the present study, heterozygous parent mice (*ctsl*$^{+/-}$) with hybrid background C57BL/6 × 129 were bred to obtain *ctsl*$^{-/-}$ and *ctsl*$^{+/+}$ littermates. For age determination of the experimental animals, females because of delivery were checked at least three times daily by the authors and by professional animal caretakers. Newborns with obscure time points of birth were omitted from the experiments. Representative tissue samples were harvested from dorsum skin only of *ctsl*$^{-/-}$ and wild-type (*ctsl*$^{+/+}$) mice at various stages during hair morphogenesis.[47] These included; day of birth (P0), day 2 (P2), day 6 (P6), day 14 (P14), day 17 (P17), day 20 (P20), and day 28 (P28) postpartum. Per genotype (*ctsl*$^{-/-}$, *ctsl*$^{+/+}$), two to three mice, each from different litters, were analyzed from each age group. Because reliable sex determination in very young mice is difficult in practice, sex was not determined in newborn, day 2 (P2), or day 6 (P6) mice. For older mice each group contained a mixture of males and females. Again, in the various *ctsl*$^{-/-}$ strains that we have obtained so far, no differences of hair cycle kinetics between males and females have been observed. There is no evidence to suggest any sex difference is present at least until P25 of age.

High-Resolution Light Microscopy (HRLM) and Transmission Electron Microscopy (TEM)

Tissues were immediately fixed in half-strength Karnovsky's fixative,[48] postfixed in 2% osmium tetroxide and uranyl acetate, and embedded in resin as previously described.[49,50] Semi- and ultra-thin sections were cut with a Reichart-Jung microtome (Vienna, Austria); the former were stained with the metachromatic stain, toluidine blue/borax, examined by light microscopy, and photographed (Leitz, Wetzlar, Germany). Loss of metachromasia from the dermal or follicular papilla was used as a marker for early catagen.[51] Ultra-thin sections were stained with uranyl acetate and lead citrate,[49] and examined and photographed using a Jeol 1200EX transmission electron microscope (Jeol, Tokyo, Japan).

Multiple blocks were examined from multiple mice at each harvesting day to generate a total of 27 blocks from *ctsl*$^{-/-}$ mice and 15 from *ctsl*$^{+/+}$ mice. Three-mm long and 1-μm thick sections were examined by light microscopy from each block. Each HRLM section contained ~15 to 20 HFs. Tissue blocks were further examined by TEM with each ultra-thin section (1.2 mm across) containing ~5 to 8 HFs.

Double Immunodetection of Terminal dUTP Nick-End Labeling (TUNEL) and Ki67-Positive Cells

Apoptotic cells were detected using an established, commercially available, TUNEL kit (ApopTag; Oncor, Gaithersburg, MD, USA) as previously described.[45] For double-immunofluorescence detection of TUNEL-positive cells and Ki67-IR, the protocol for the TUNEL technique was combined with the manufacturer's protocol for Ki67-immunohistochemistry.[44] Briefly, 4-μm sections were deparaffinized and heated in citrate buffer, pH 6.0, for 5 minutes at 100°C and then incubated with rabbit anti-Ki67 antiserum followed by an incubation with digoxigenin-dUTP in the presence of TdT. Subsequently, TUNEL-positive cells were visualized by anti-digoxigenin fluorescein isothiocyanate-conjugated $F(ab)_2$ fragments, Ki67-IR was detected by goat anti-rabbit tetramethylrhodamine B isothiocyanate-conjugated antibody, and the sections were counterstained by Hoechst 33342. Negative controls for the TUNEL staining omitted TdT, according to the manufacturer's protocol. Positive TUNEL controls were as described[45] by comparison with tissue sections from the thymus of infantile mice, which display a high degree of spontaneous thymocyte apoptosis.[52]

After washing in phosphate-buffered saline (PBS), all sections were mounted with immunomount medium (Shandon, Pittsburgh, PA, USA). Sections were examined under a Zeiss Axioscope microscope, using the appropriate excitation-emission filter systems for fluorescence, induced by Hoechst 33342, fluorescein isothiocyanate, or tetramethylrhodamine b isothiocyanate. Photodocumentation was by a digital image-analysis system (ISIS Metasystems, Altlussheim, Germany).

Immunohistochemical Detection of Trichohyalin

Tissue was taken from mice during various stages of HF morphogenesis as indicated above and frozen for cyrosectioning. Four-μm sections were fixed in acetone at −20 C° for 10 minutes, rehydrated, and equilibrated in PBS for 10 minutes at room temperature. Tissue sections were then blocked with avidin, biotin, and 10% normal goat serum and incubated overnight with a mouse monoclonal antibody to trichohyalin (AE15), diluted 1:200 (a gift from Prof. T-T Sun, NYU Medical Center, New York, NY). This was followed after washing by incubation with goat anti-mouse secondary antibody diluted 1:100 for 1 hour at room temperature. Alkaline phosphatase was used as the chromogen (AEC kit; DAKO, Glostrup, Denmark). Sections were counterstained by hematoxylin and mounted with Kaiser's glycerine.

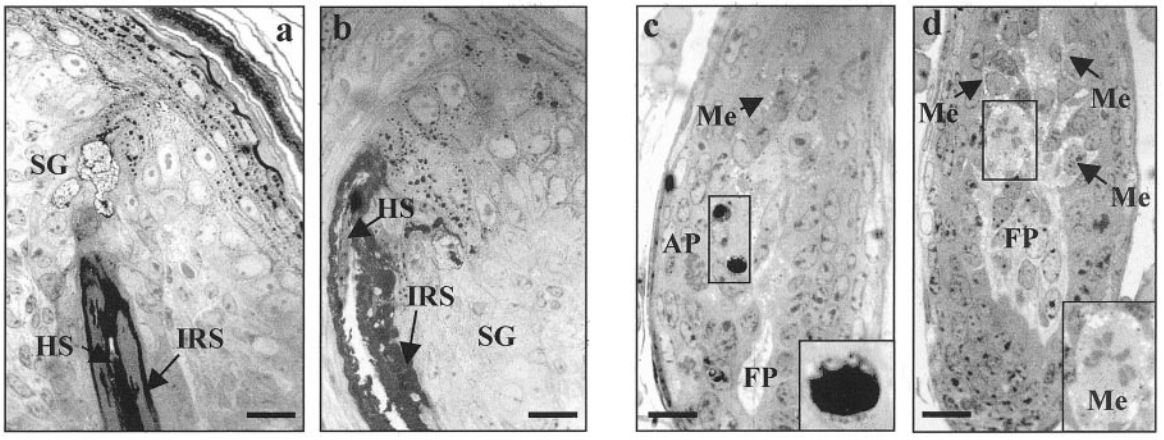

Figure 1. HF morphogenesis: defective development of HFs in *ctsl*$^{-/-}$ mice. **a:** Distal region of stage 5 *ctsl*$^{+/+}$ HF showing normal IRS development characterized by a straight and symmetrical arrangement of fully keratinized hair cone/IRS cells. The hair cone/IRS is degraded proximal to the sebaceous gland (SG). **b:** Distal region of stage 5 *ctsl*$^{-/-}$ HF showing abnormal IRS development characterized by a highly ruffled and thickened hair cone/IRS that is retained beyond the level of the sebaceous gland (SG). **c:** Proximal regions of stage 5 *ctsl*$^{-/-}$ HF showing premature apoptosis in the hair bulb (AP). **Inset**: Higher power view of apoptotic melanocyte. Note pigment granules. **d:** Proximal region of stage 5 *ctsl*$^{-/-}$ HF showing marked vacuolation of differentiating and proliferating hair bulb melanocytes. HRLM, toluidine blue. Scale bars: 10 μm (**a** and **b**); 15 μm (**c** and **d**).

Results

The current study evaluated the effect of CTSL deficiency on hair morphogenesis and the subsequent first hair cycle in mice using an integrated morphological and cell kinetics approach. Postnatal HF morphogenesis and cycling in *ctsl*$^{+/+}$ mice proceeded through the developmental stages of induction, organogenesis, cytodifferentiation, and subsequent cyclic transformations as previously described.[53–55] By contrast, deficiency in this lysosomal protease resulted in striking abnormalities in HF development and cycling of HF.

The Formation of the Hair Canal Is Abnormal in Developing ctsl$^{-/-}$ *Mice*

Despite the recognized retardation of HF development in *ctsl*$^{-/-}$ mice,[17] both *ctsl*$^{+/+}$ and knockout mice exhibited similar HF morphology on day of birth (P0). In this regard, the back skin of both *ctsl*$^{+/+}$ and *ctsl*$^{-/-}$ mice contained HFs in all developmental stages up to, but not including, the development of the hair canal (stage 5). The earliest morphological abnormality in *ctsl*$^{-/-}$ mice (*ctsl*$^{-/-}$) was apparent at P2 in stage 5 HFs. At this stage in HF morphogenesis, *ctsl*$^{+/+}$ HFs contained an easily recognizable sebaceous gland, although the tip of the growing hair shaft was still confined within a straight and symmetrical IRS.[53] However, no clear hair/pilary canal was yet apparent (Figure 1a). By contrast, the developing IRS in *ctsl*$^{-/-}$ HF exhibited marked twisting associated with defective development of the hair canal, apparently because of abnormal hardening/differentiation and abnormal desquamation of the IRS-like hair cone cells (Figure 1b). The IRS-like hair cone cells exhibited striking structural abnormality characterized by considerable ruffling and twisting such that cohesion with the emerging hair shaft was lost. Furthermore, the association between the developing hair infundibulum and the developing sebaceous gland was abnormal. The newly formed duct of the sebaceous gland exited externally to the developing hair shaft rather than opening directly into the hair canal. A preferential and sequential degradation of these structures during hair canal formation is needed for optimal spatial configuration of the sebaceous duct.[56]

Abnormally High Levels of Keratinocyte and Melanocyte Apoptosis Occur in the Developing ctsl$^{-/-}$ *HF*

HRLM and TEM analysis revealed that premature keratinocyte and melanocyte apoptosis was common throughout the developing stage 5 hair bulb. Dying cells were located predominantly above the proliferative region of the sub-Auber's hair bulb (Figure 1c). Some apoptotic cells were clearly melanocyte in origin, as evidenced by their containing some melanized melanosomes at a stage of HF development that precedes transfer of melanin granules to precortical keratinocytes. Apoptosis was rarely seen in stage 5 hair bulb of *ctsl*$^{+/+}$ skin. Thus, HF morphogenesis in *ctsl*$^{-/-}$ mice is associated with increased levels of cell death (via apoptosis) and involved both keratinocyte and melanocyte subpopulations.

Development of the HF Pigmentary Unit in Developing HFs Is Perturbed by the Absence of CTSL

Melanocytes migrated successfully to the upper hair bulb matrix around the follicular papilla in stage 5 HFs of both *ctsl*$^{+/+}$ and *ctsl*$^{-/-}$ HFs. However, as alluded to above, some melanocytes that had commenced melanosome organellogenesis and melanogenesis were deleted by apoptosis in *ctsl*$^{-/-}$ HF (Figure 1c). These deleted cells may have been replaced by local melanocyte proliferation, as the total complement of melanocytes in fully developed (stage 8) *ctsl*$^{-/-}$ hair bulbs appeared normal

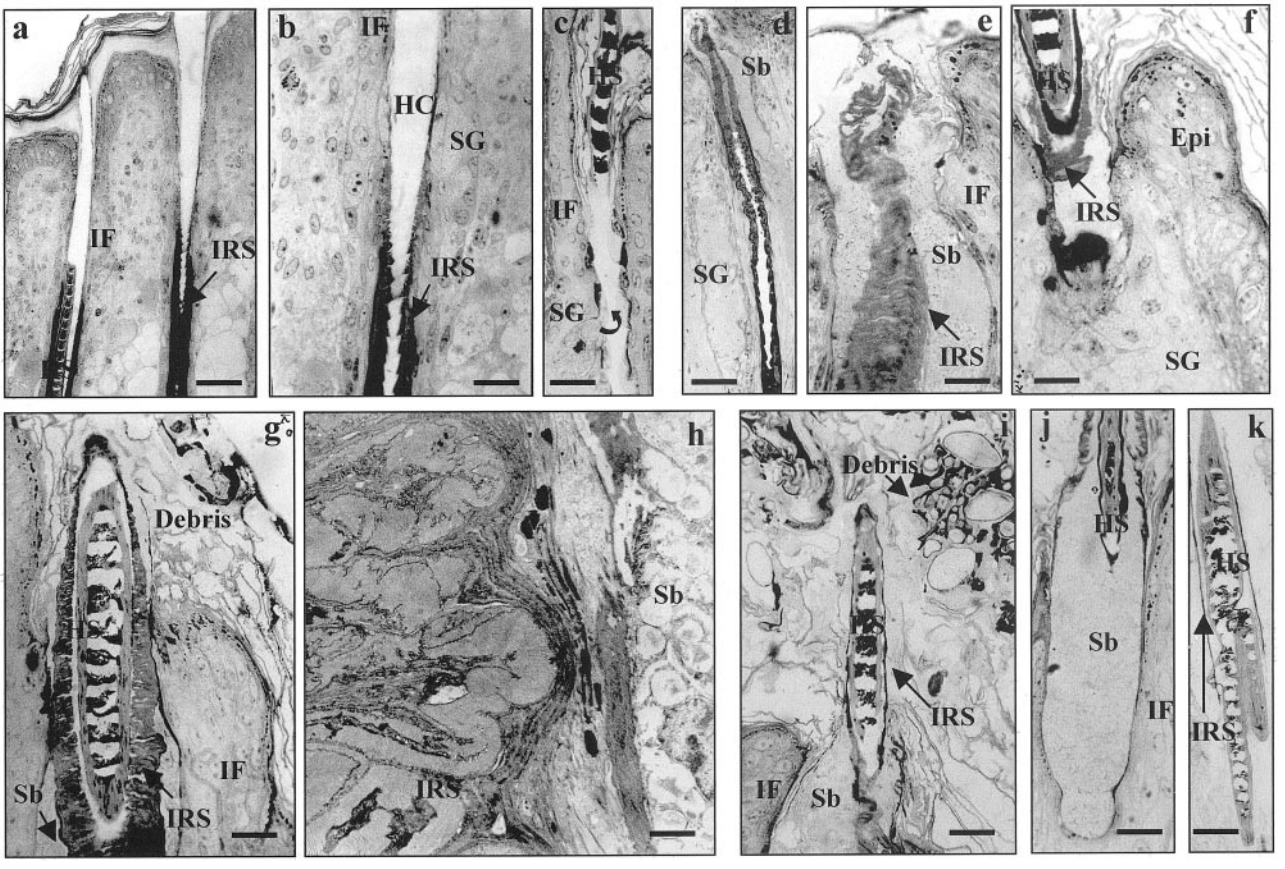

Figure 2. HF morphogenesis: defective hair shaft exiting in *ctsl*$^{-/-}$ mice. **a:** Distal region of a fully developed stage 5 *ctsl*$^{+/+}$ HF showing normal hair canal and infundibulum structure characterized by the gradual loss/degeneration of IRS at the level of the sebaceous gland. Note that the hair canal is only sufficiently wide to permit passage of the hair shaft. **b:** Higher power view of the gradual thinning/disintegration of the IRS close to the sebaceous gland (SG). Note that the hair canal (HC) is clear of debris. **c:** Infundibular region (IF) of a fully developed stage 5 *ctsl*$^{+/+}$ HF showing the exiting point of sebaceous gland (SG) products, via the sebaceous duct (**arrow**), into the hair canal. Note the absence of IRS material at this level of the hair canal; hair shaft (HS). **d:** Distal region of fully developed *ctsl*$^{-/-}$ HF showing the retention of IRS above the level of the sebaceous gland (SG) and its emergence through to the skin surface. **e:** Higher power view of distal-most region shown in **d**. The opening of the HF appears blocked with sebum-like material. This is removed from the HF external to the IRS rather than along the hair shaft (HS) as occurs in normal *ctsl*$^{+/+}$ mice. **f:** Distal region of fully developed *ctsl*$^{-/-}$ HF showing a sebaceous gland (SG) opening at the skin surface (Epi). Note that intact sebocytes lining the surface of the infundibulum with apparent disrupted holocrine secretion. A hair shaft (HS) encased in IRS material is present in this HF. **g:** Distal region of fully developed *ctsl*$^{-/-}$ HF showing the emergence of the hair shaft to the skin surface associated with considerable amounts of IRS-derived material. Sebum-like material is located external to the IRS hair shaft (HS) complex and is associated with the dilation of the hair canal and increased debris on the skin surface. **h:** Higher power view of IRS material at level of sebaceous gland (SG). Note that this ectopic material exhibits a typical IRS cell morphology including the retention of nuclear ghosts, although lacks evidence of IRS cuticle. **i:** Distal region of fully developed *ctsl*$^{-/-}$ HF showing the exiting of the hair shaft (HS) from the skin surface. Note the retention of IRS-derived material around the hair shaft and the considerable amounts of debris. **j:** Distal region of fully developed *ctsl*$^{-/-}$ HF showing the exiting of the hair shaft (HS) from the skin surface. Note the marked dilation of the hair canal, a fully sixfold increase over the hair shaft (HS) diameter. The hair canal is also clogged with sebum-like material (Sb). **k:** Defective hair shaft (HS) located on the skin surface of *ctsl*$^{-/-}$ mice. Note the retention of IRS-derived material around the bifurcated hair shaft with severe twisting of the hair cortex. HRLM: toluidine blue. TEM (**g**): uranyl acetate and lead citrate. Scale bars: 50 μm (**a**), 15 μm (**b**, **e–g**, **j**, and **k**), 30 μm (**c**), 60 μm (**d**), 2 μm (**h**), 20 μm (**i**).

(ie, consisted of one melanocyte to five keratinocytes in the hair bulb as a whole and 1:1 in the basal layer of the hair bulb next to the follicular papilla).[57] However, additional melanocyte defects were evident, including marked vacuolation specific for bulbar melanocytes. This defect was not found in neighboring bulbar keratinocytes or indeed in the amelanotic melanocytes located in the outer root sheath of the HF. This massive vacuolation was associated only with the early stages in the biogenesis of the lysosome-derived melanosomes (Figure 1d) and seemed to be transient. Despite melanocyte apoptosis and vacuolation of surviving bulbar melanocytes, a full complement of melanocytes was present in *ctsl*$^{-/-}$ hair bulbs, such that stage 8 hair bulbs appeared to be similarly pigmented in both *ctsl*$^{+/+}$ and *ctsl*$^{-/-}$.

Exiting of Hair Shafts to the Skin Surface Is Impaired in ctsl$^{-/-}$ *HFs*

Ctsl$^{-/-}$ mice exhibited defective exiting of hair shafts from the hair canal. Twisting of the hair cone and IRS in stage 5 to 6 *ctsl*$^{-/-}$ HFs (day P2) was associated with the aberrant development of HF canals and infundibula. Such changes seemed to restrict the normal exiting of growing hair shafts. By contrast, the formation of hair canals in *ctsl*$^{+/+}$ mice was characterized by the regular desquamation of IRS cells just below the exit point of the sebaceous duct. This duct channeled sebaceous gland-secreted products directly into the hair canal (Figure 2; a to c). Such proteolysis/desquamation of IRS in *ctsl*$^{+/+}$

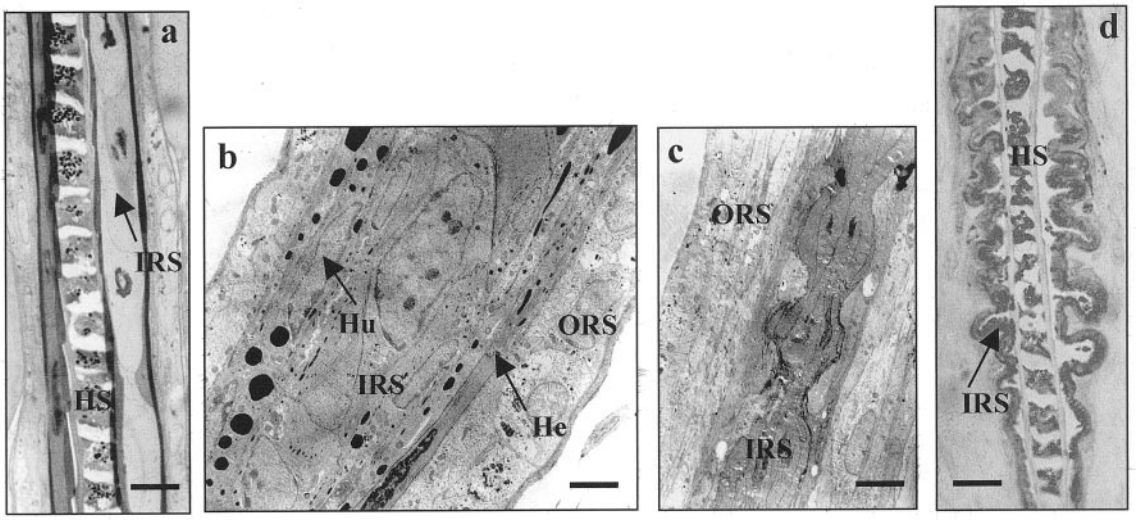

Figure 3. HF morphogenesis: defective formation and differentiation of the HF's IRS in *ctsl*$^{-/-}$ mice. **a:** Mid region of a fully developed *ctsl*$^{-/-}$ HF showing IRS asymmetry. Note the reduced volume of IRS ensheathing part of the hair shaft (HS). Note also the relatively normal imbrication pattern of the IRS cuticle and associated hair shaft cuticle. **b:** High-power view of variable differentiation in the IRS ensheathing part of the developing *ctsl*$^{-/-}$ hair shaft (HS). Note that keratinization of Henle's layer (He) is more advanced on the right than the left side of this sectioned HF. Hu, Huxley's layer of IRS. **c:** Defective IRS differentiation/keratinization in *ctsl*$^{-/-}$ HF. Note that the IRS is highly contorted with apparent twisting/torsion. **d:** Defective IRS at the level of the sebaceous gland in *ctsl*$^{-/-}$ HF. Note that the IRS is highly folded and lacks a discrete cuticular layer resulting in the loss of imbrication with the hair shaft. HRLM (**a** and **c**): toluidine blue; TEM (**b** and **d**): uranyl acetate. Scale bars: 15 μm (**a** and **d**), 5 μm (**b**), 10 μm (**c**).

HFs resulted in the progressive and gradual thinning of the distal IRS, until it disappeared as a distinct component above the level of the sebaceous gland (Figure 2, a and b). In *ctsl*$^{+/+}$ HFs, holocrine sebaceous gland secretions emptied directly into the hair canal from the sebaceous gland via a specialized duct (Figure 2c). This structural arrangement of the upper pilosebaceous unit was associated with the emerging hair shaft occupying fully the hair canal space. By contrast, the IRS of *ctsl*$^{-/-}$ HFs neither hardened fully nor desquamated at the appropriate level close to the sebaceous gland (Figure 2; d to g). Instead, this HF component was retained in the distal hair canal to disrupt the normal flow of the sebaceous gland's secretions into the hair canal (Figure 2, d and e). The resultant accumulation of sebaceous gland products clogged the hair canal (Figure 2; d to i).

Persistent disruption of hair shaft exiting in *ctsl*$^{-/-}$ mice correlated with the accumulation of increasing amounts of heterogeneous debris consisting of disorganized hair shaft, stratum corneum, and sebum material at the epidermis surface (Figure 2, g and i). The epidermal surface of *ctsl*$^{+/+}$ mice was clear by comparison (similar to that shown in Figure 2a). A net effect of delayed IRS differentiation and desquamation in *ctsl*$^{-/-}$ mice was the emergence of hair shafts from the hair canal encased by IRS-like material. This contributed an additional twofold to threefold increase in the diameter of the hair shaft/IRS complex within the hair canal (Figure 2g). To accommodate this change, the hair canal in *ctsl*$^{-/-}$ mice was commonly dilated by up to sixfold compared to *ctsl*$^{+/+}$ mice (Figure 2, g and i). The IRS origin of much of this material was evidenced by its retained features of incomplete IRS differentiation, ie, characteristic nuclear remnants (Figure 2h).

A range of related structural defects were also seen in the hair shaft including bifurcation and twisting of hair cortex (Figure 2k). A possible origin of these distal defects was apparent more proximally in the *ctsl*$^{-/-}$ HF with the asymmetric differentiation of the IRS. The rate of IRS cell differentiation was often markedly unequal on both sides of the follicle (Figure 3, a and b). Below the level in which the IRS normally desquamates (ie, at sebaceous gland), the IRS in *ctsl*$^{-/-}$ mice exhibited apparent torsion effects (Figure 3c). This defect resulted, more distally, in the production of highly ruffled forms whereby the IRS retained only partial contact with its ensheathed hair shaft (Figure 3d).

Although *ctsl*$^{-/-}$ sebaceous gland products did exit the HF, this occurred external to the IRS material, and therefore external to the hair shaft (Figure 2; d to g). Thus, the absence of CTSL strikingly disrupts the normal proteolysis/desquamation of the hair shaft-molding IRS. This results in the abnormal exiting of not only the hair shaft, but also of sebaceous gland products that normally lubricate the emerging hair shaft. No obvious alteration in the outer root sheath (OTS) was apparent (Figure 3, a and b).

Sebaceous Gland Development Appears to Be Normal in ctsl$^{-/-}$ *HFs*

No significant defects in sebaceous gland morphogenesis were detected in *ctsl*$^{-/-}$ mice. However, sebaceous glands appeared to be located unusually high in the dermis in *ctsl*$^{-/-}$ HFs, where their apical surface commonly opened directly into the HF infundibulum rather than via a sebaceous duct (Figure 2f). Sebocyte differentiation appeared normal in all of the *ctsl*$^{-/-}$ mice studied.

CTSL Deficiency Retards HF Regression (Catagen)

HF regression (catagen) was well-advanced in *ctsl*$^{+/+}$ skin by P17, where it was associated with high levels of apoptosis in defined HF compartments (Figure 4a).[45] In these normal mice, club formation occurred only after advanced regression in the lower two-thirds of the HF (ie, when the HF had involuted and retracted to just below the sebaceous gland). Moreover, the hair canal of catagen *ctsl*$^{+/+}$ HFs was only sufficiently wide to permit easy and clear movement of the hair shaft, which was otherwise moored firmly in the telogen HF. By contrast, in *ctsl*$^{-/-}$ mice catagen was both delayed and defective (Figure 4b). Many HFs were still in full anagen as evidenced by their continued hair bulb melanogenesis, absence of apoptosis, and their location deep in the hypodermis close to the panniculus carnosus (Figure 4b).

CTSL Deficiency Truncates the HF Resting (Telogen) Phase

By P20, all *ctsl*$^{+/+}$ HFs were in the telogen phase (Figure 4, c and d). Telogen club formation exhibited characteristic features including the cessation of IRS differentiation (ie, discrete Henley's and Huxley's layers were no longer apparent) and advanced formation of telogen club rootlets that anchor telogen clubs to the HF (Figure 4g). By contrast, *ctsl*$^{-/-}$ mice contained many HFs that were still located deep in the subcutis, evidently undergoing a delayed involution process (Figure 4, e and f). This morphology corresponded well with reduced catagen-associated apoptosis as assessed by both ultrastructural analysis (Figure 4, e and f) and by TUNEL histomorphometry (Figure 6, a and b). Furthermore, club hair formation in *ctsl*$^{-/-}$ catagen follicles was aberrant and occurred before significant catagen-associated HF shortening, ie, while HFs were still extended deep into the corium (Figure 4, e and f). *ctsl*$^{-/-}$ club formation also appeared to occur before the cessation of IRS cell differentiation, as indicated by the continued presence of a differentiating Huxley's layer (Figure 4h). Despite delayed catagen in *ctsl*$^{-/-}$ mice, no telogen HFs were present at P28 (Figure 4j), ie, a time when *ctsl*$^{+/+}$ HFs were predominantly in telogen (Figure 4; c, d, and g), using standardized morphological criteria for HF cycle classification.[55] Rather, the back skin of *ctsl*$^{-/-}$ mice was already in anagen V. Indeed, anagen III/IV HFs were present as early as P22 in some *ctsl*$^{-/-}$ mice (Figure 4i).

CTSL Deficiency Facilitates the Premature Shedding of Hair Shafts

The infundibula of cycling *ctsl*$^{-/-}$ HFs were still highly dilated and contained much sebaceous-derived and IRS material inherited from the preceding HF development phase (Figure 4; i to k). An induced exogen phase resulted in the shedding of apparently poorly anchored club hairs from these anagen-cycling HFs (Figure 4, i and j). However, the vacated hair canals remained dilated and clogged with heterogeneous material, including sebum-like products. In contrast to hair morphogenesis, a discrete but heavy inflammatory cell infiltrate was observed around, but not within, sebaceous glands. By TEM and HRLM analysis, these consisted primarily of eosinophils, neutrophils, and macrophages (Figure 4l).

CTSL Deficiency Precipitates a Premature Entry into the First Growth (Anagen) Phase

The absence of CTSL significantly delayed the apoptosis-driven regression of the *ctsl*$^{-/-}$ catagen HF, although apparently not the initial stages of club formation. Soon after the regressing HFs entered the resting telogen phase of the hair cycle they were prematurely precipitated into hair regrowth (anagen) and soon thereafter shed their club hairs (Figure 4; i to k). This hair shaft shedding phase or exogen occurred before the onset of HF melanogenesis in anagen III/IV,[58] ie, approximately between P19 and P22. Moreover, the hair canals remained blocked throughout with maintained disruption of the normal sebaceous gland secretion apparatus (Figure 4k).

To investigate HF cell proliferation and death in *ctsl*$^{-/-}$ cycling HFs, we counted the number of Ki67-positive cells (proliferation marker) (Figure 5a1) and TUNEL-positive cells (apoptosis marker) (Figure 5a2). *Ctsl*$^{-/-}$ backskin HFs contained more proliferating cells than *ctsl*$^{+/+}$ HF at identical stages. Quantitative analysis of Ki67-positive cells showed an increase in HFs of *ctsl*$^{-/-}$ mice compared to *ctsl*$^{+/+}$ littermates (Figure 5a1). Although no significant difference in numbers of proliferating keratinocytes could be detected in anagen VI hair bulbs between *ctsl*$^{+/+}$ and *ctsl*$^{-/-}$ mice, the latter did show a significant increase in numbers of Ki67-positive cells in the area of the infundibulum during anagen VI, catagen, and telogen (Figure 5b; 2, 4, and 6). Cell proliferation in regenerating anagen *ctsl*$^{+/+}$ HFs was predominantly localized in the proximal hair bulb region (Figure 5b1), whereas *ctsl*$^{-/-}$ HF exhibited high rates of proliferation throughout the entire epithelium (Figure 5b2). Keratinocyte proliferation was significantly higher in *ctsl*$^{-/-}$ *versus* *ctsl*$^{+/+}$ upper HFs (Figure 5b, 3 and 4). Similarly, significantly increased keratinocyte proliferation was apparent in anagen, catagen, and telogen *ctsl*$^{-/-}$ *versus* *ctsl*$^{+/+}$ HFs (Figure 5b; 2, 4, and 6). Overall, cell proliferation was twofold higher in *ctsl*$^{-/-}$ HFs compared to the *ctsl*$^{+/+}$ HFs (Figure 5a1).

Quantitative analysis of TUNEL-positive cells showed an decrease in HFs of *ctsl*$^{-/-}$ mice compared to *ctsl*$^{+/+}$ littermates (Figure 5a2). Although no significant difference in number of apoptotic cells was detected in catagen hair bulbs of *ctsl*$^{+/+}$ and *ctsl*$^{-/-}$ mice, the latter did show a significant decrease in numbers of TUNEL-positive cells in the area of the infundibulum during anagen VI, and catagen (Figure 5, a2 and b; 2, 4, 6).

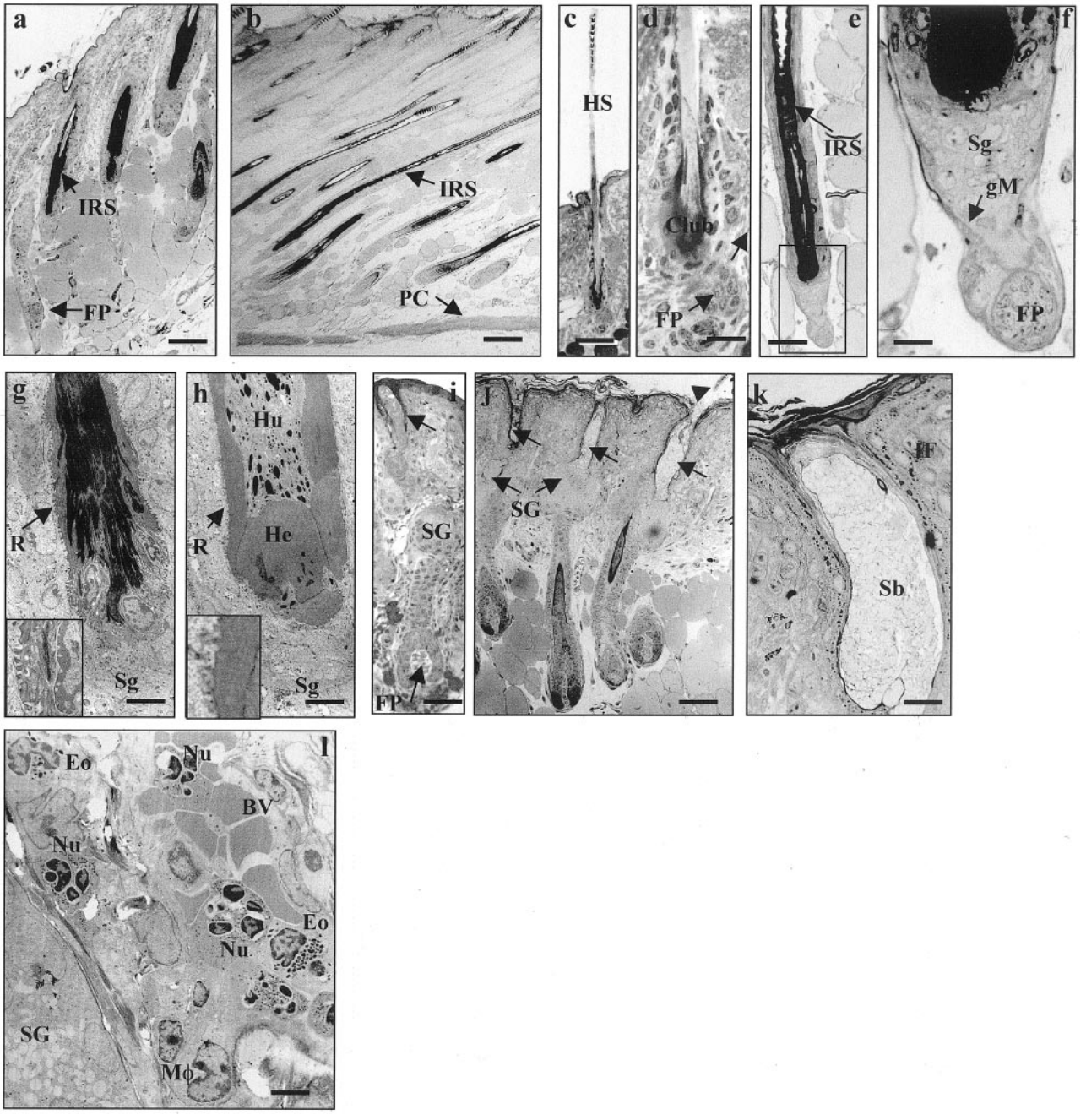

Figure 4. HF regression (catagen) to HF quiescence (telogen): defective HF cycling in *ctsl*$^{-/-}$ mice. **a:** HF regression (catagen) in *ctsl*$^{+/+}$ mice at p17 characterized by massive apoptosis in the transient lower two-thirds of the HF. Note also that hair club formation occurs high in the skin above the fat layer. **b:** Delayed entry of *ctsl*$^{-/-}$ HFs into catagen in p20 mice 3 days later than for *ctsl*$^{+/+}$ HFs in **a** above. Note that many of these HFs exhibit full anagen VI length and penetrate deep into the subcutis to the level of the muscle layer. **c** and **d:** Telogen HFs in *ctsl*$^{+/+}$ mice at p22 characterized by the presence of only the permanent upper third of the HF. The club is well anchored into the surrounding epithelial sac with the follicular papilla attached to the base (FP). **e** and **f:** Abnormal catagen in a *ctsl*$^{-/-}$ HF at p20. Note that the club forms while the proximal HF is still deep in the subcutis and before evidence of significant apoptosis, although catagen-associated changes including thickening of the glassy membrane (g) and clustering of FP cells (FP) can be seen. **g:** Hair club formation during telogen in *ctsl*$^{+/+}$ mouse at p20. Note the advanced formation of the anchoring rootlets (magnified in **inset**) and the complete keratinization of the club-forming cells and adjacent secondary germ keratinocytes (Sg). **h:** Hair club formation during telogen in *ctsl*$^{-/-}$ mouse at p20. Note the poorly formed anchoring rootlets (magnified in **inset**) and the presence of ongoing differentiation of the IRS Huxley's layer (Hu). **i:** Premature cycling into anagen III in *ctsl*$^{-/-}$ mice at p22. Note the absence of club hairs in the dilated and sebum-clogged hair canal (**arrow**) and prominent sebaceous gland (SG). **j:** Premature cycling into anagen IV/V in *ctsl*$^{-/-}$ mice at p28. Note that all hair canals were empty of club hairs, although a rare hair shaft can be seen associated with one of the hair canals (**arrowhead**). Prominent sebaceous glands (SG) and associated with hair canals were clogged with sebum-like material. The morphology of the cycling anagen HF appears normal at this stage. **k:** High-power view of an infundibulum blocked with apparent sebum-like material (Sb). Note the absence of the hair shaft. **l:** Leukocyte infiltration around (but not within) the sebaceous glands of cycling anagen V *ctsl*$^{-/-}$ HF. These perivascular (BV) infiltrates consisted predominantly of granulocytes including eosinophils, neutrophils, and macrophages. HRLM (**h–f**, **i**, and **j**): toluidine blue. TEM (**g**, **h**, and **k–o**): uranyl acetate and lead citrate. Scale bars: 90 μm (**a** and **c**), 100 μm (**b**), 30 μm (**d**), 60 μm (**e**), 15 μm (**f** and **k**), 5 μm (**g** and **h**), 50 μm (**i**), 70 μm (**j**).

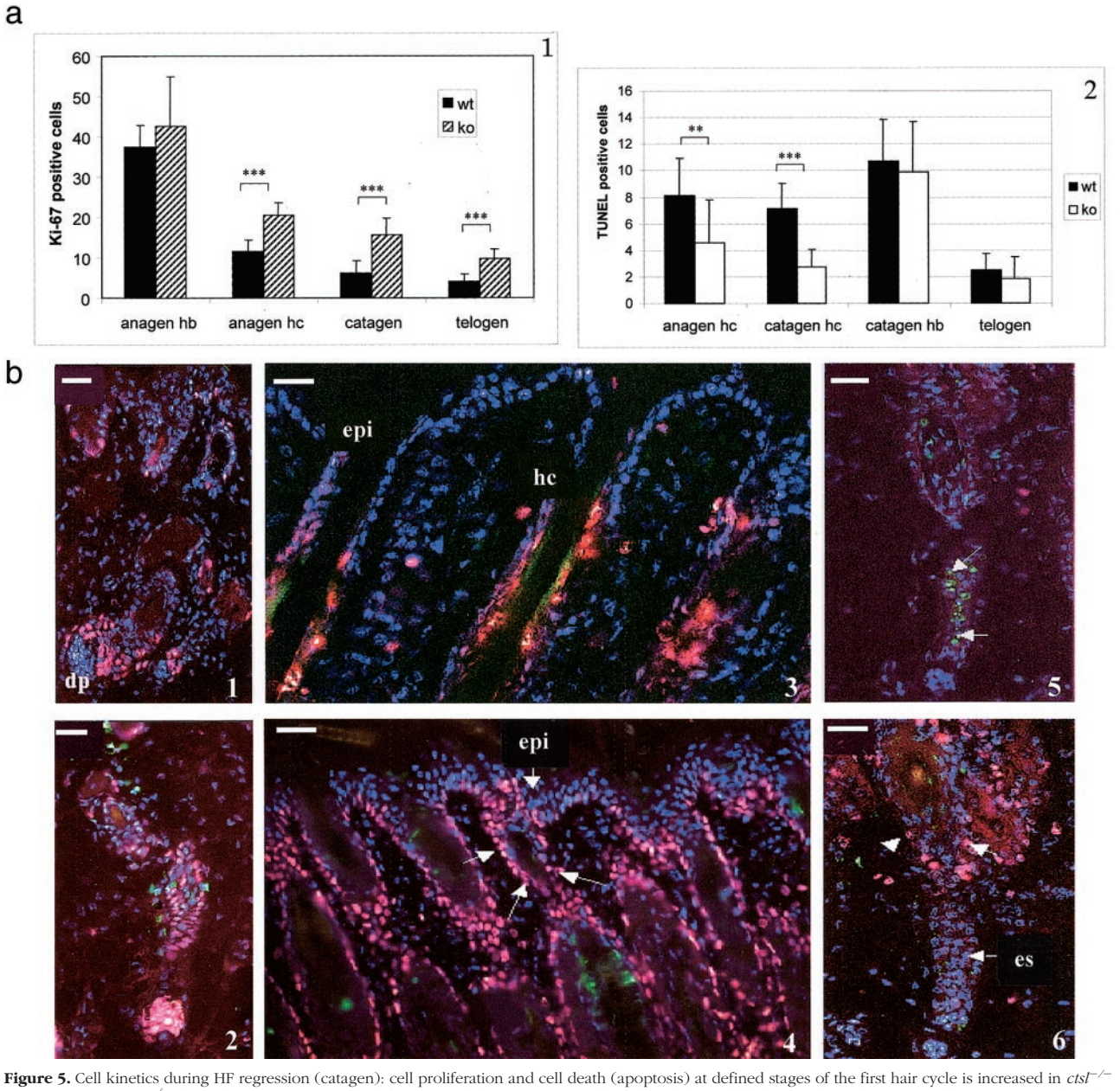

Figure 5. Cell kinetics during HF regression (catagen): cell proliferation and cell death (apoptosis) at defined stages of the first hair cycle is increased in $ctsl^{-/-}$ mice. **a:** HFs in $ctsl^{-/-}$ back skin contain more proliferating and less apoptotic cells than wild-type follicles at identical stages. Cells were counted in the infundibulum region around the hair canal (hc) and in the hair bulb (hb). **a1:** Quantitative analysis of Ki67-positive cells shows an increase in HF of $ctsl^{-/-}$ mice compared to $ctsl^{+/+}$ littermates during the complete hair cycle. Compared to the $ctsl^{+/+}$ (**black bar**) mice $ctsl^{-/-}$ mice, (**dashed bar**) show a significant twofold increase of Ki67-positive cells in catagen and telogen back skin HFs (n = 3 to 5 mice/group). A significantly higher number of Ki67-positive cells occur in the distal anagen HF in $ctsl^{-/-}$ mice. By contrast, no difference could be detected in the hair matrix and follicular papilla (FP). **a2:** Quantitative analysis of TUNEL-positive cells in anagen VI, catagen, and telogen HF of $ctsl^{-/-}$ mice (**white bar**) *versus* $ctsl^{+/+}$ mice (**black bar**). Significantly lower levels of TUNEL-positive cells were detected in HF of $ctsl^{-/-}$ mice compared $ctsl^{+/+}$ mice in the same hair cycle stage (n = 3 mice/group). Significance was calculated by unpaired two-tailed Student's t-tests. *, $P = 0.5$; **, $P = 0.01$; ***, $P = 0.001$. **b:** Cryostat sections of $ctsl^{-/-}$ and $ctsl^{+/+}$ mice back skin were processed for the double immunovisualization of Ki67 (pink) and TUNEL (green) and counterstained with Hoechst (blue). **b1:** Anagen II $ctsl^{+/+}$ HF. Proliferating keratinocytes close to the follicular papilla (FP) and only scattered cells in the distal HF show Ki67 positivity (red immunofluorescence). **b2:** Anagen II $ctsl^{-/-}$ HF. Note the greater number of Ki67-positive cells throughout the entire HF. **b3:** Anagen VI hair $ctsl^{-/-}$ HF. Note that the infundibular region contains significantly more Ki67-positive and more TUNEL-positive (green) cells compared to $ctsl^{+/+}$ HFs. **b4:** Anagen VI $ctsl^{+/+}$ HF. Note that only scattered keratinocytes in the basal layer of the epidermis (epi) and around the hair canal are Ki67-positive. **b5:** Catagen VII $ctsl^{-/-}$ HF. Note that proliferating cells (red) are detectable in the lower portion of the HF. **b6:** Catagen VII $ctsl^{+/+}$ HF. Note that no Ki67-positive cells can be detected in the HF. Several apoptotic nuclei can be seen in the epithelial strand (**arrows**, es). fp, Follicular papilla; epi, epidermis; hc, distal HF around hair canal; es, epithelial strand. Scale bars, 30 μm (**b1–b6**).

Melanocytes and Keratinocytes of Cycling ctsl$^{-/-}$ *HFs Exhibit Specific Abnormalities*

As with HF morphogenesis, marked cytoplasmic vacuolation was present in hair bulb melanocytes in the regenerating anagen HF pigmentary unit (Figure 6; a to e). Moreover, this defect was again associated with the commencement of melanosome organellogenesis. Some reduction in the number of melanogenically active hair-bulb melanocytes was apparent in some HFs (Figure 6c),

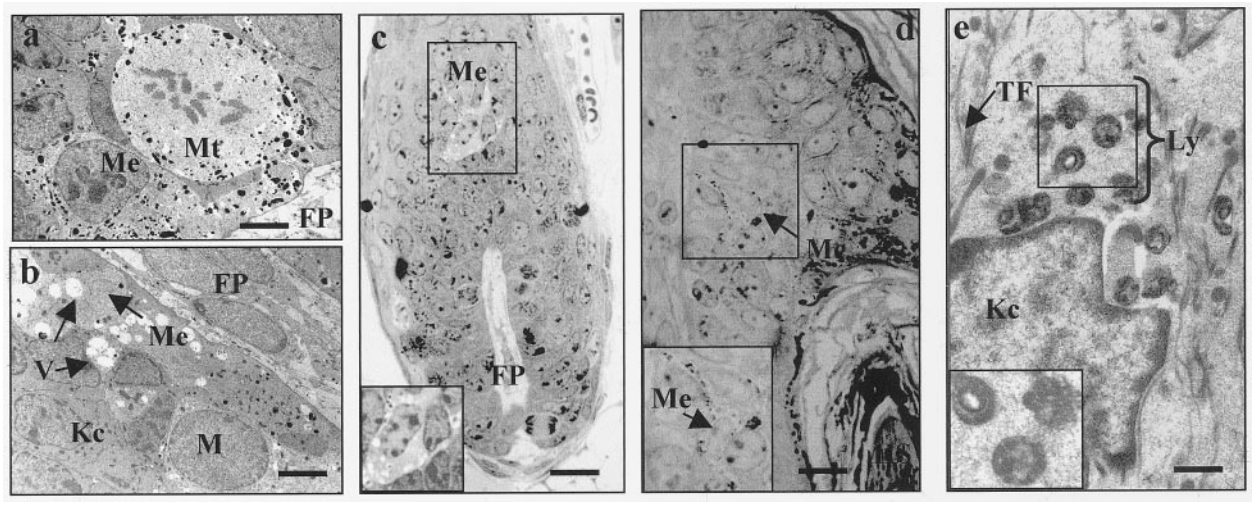

Figure 6. HF melanocyte status: defects in lysosome-related organelles in *ctsl*$^{-/-}$ mice. **a** and **b:** Pigmentation perturbations in *ctsl*$^{-/-}$ anagen V HFs at p28. Melanocytes exhibited marked vacuolation both as mitotic (mt) and interphase (me) cells. Note that not all melanocytes are similarly affected (m). **c:** Apparent reduction in melanocyte repopulation during regeneration of hair pigmentary unit in cycling *ctsl*$^{-/-}$ HF. Note that only a single differentiated melanocyte (Me) is readily apparent in the supra-FP region (FP) of the hair bulb. Note also, that this cell also exhibits considerable cytoplasmic vacuolation. **Inset**: High-power view of a vacuolated melanocyte. **d:** Induction of melanogenesis in epidermal melanocytes during *ctsl*$^{-/-}$ HF development at p14. Note the presence of two clear cells (**arrow**), one of which is highly dendritic and contains numerous melanin granules. Note also proximity to the hair shaft (HS). **Inset**: High-power view of melanogenically active epidermal melanocyte. **e:** Increased formation of lysosomes within differentiating hair bulb precortical keratinocytes in a *ctsl*$^{-/-}$ HF at p28. These lysosomes were located in clusters in some, but not all, differentiating keratinocytes. **Inset**: High-power view of unusual lysosome-like structures. HRLM (h–f, i, and j): toluidine blue. TEM (g, h, k–o): uranyl acetate and lead citrate. Scale bars: 2.5 μm (**a**), 4 μm (**b**), 20 μm (**c**), 1.5 μm (**d**), 8 μm (**e**).

although this was not quantified. In addition to melanosome defects, differentiating hair-bulb precortical keratinocytes in regenerating anagen HFs contained numerous lysosome-like structures not detected during HF morphogenesis (Figure 6e). Thus, melanocyte and precortical keratinocyte populations may accumulate defects during HF morphogenesis and the first genuine hair cycle. Melanogenically active melanocytes were occasionally located close to the HF infundibulum and were identified by their pigment content and dendricity (Figure 6d). Melanogenic melanocytes are not usually present in the distal epithelium of murine truncal skin.[58–60]

Trichohyalin Expression Is Altered in ctsl$^{-/-}$ *Mice*

Many of the morphological abnormalities in *ctsl*$^{-/-}$ HF pertained to the IRS. To assess the effect of CTSL deficiency on the formation, differentiation, and disintegration of this HF component, the expression of a major and characteristic IRS structural protein, trichohyalin, was examined. Immunohistochemistry used the AE15 antibody[59] that reacted with the granule-limited form of this protein. *ctsl*$^{+/+}$ and *ctsl*$^{-/-}$ expression of this polymeric protein was detected in the proximal IRS during late catagen (IV to V) in P19 mice. Expression was lost during more advanced catagen (ie, VI to VIII) and remained absent during telogen and early anagen (I to II). Trichohyalin expression reappeared at anagen III, coinciding with the onset of IRS cell differentiation.[54] The distribution of trichohyalin expression was similar in both *ctsl*$^{-/-}$ and *ctsl*$^{+/+}$ mice. However, the intensity of immunostaining was weaker in *ctsl*$^{-/-}$ anagen VI HFs (Figure 7a) than in the anagen VI *ctsl*$^{+/+}$ HFs (Figure 7b). Thus, the absence of CTSL correlated with a reduced expression of the major IRS structural protein, trichohyalin.

Discussion

Recent evidence has implicated an important role for protease/anti-protease systems in the control of the extensive tissue remodeling that occurs during HF cycling.[1–3,9–16] CTSL is the first lysosomal proteinase

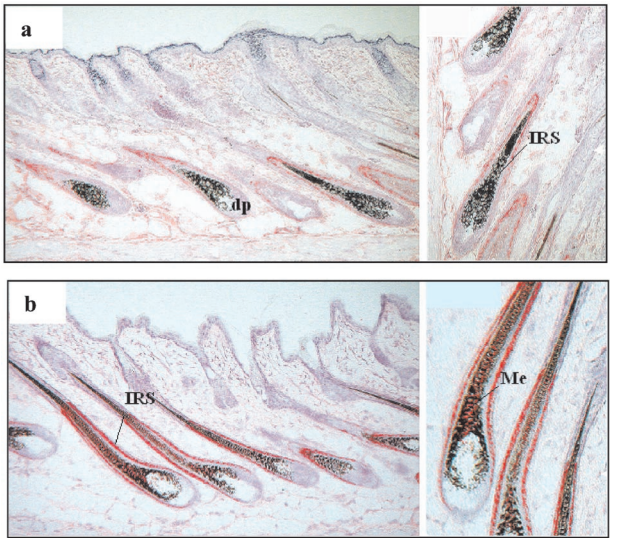

Figure 7. Reduced expression of the IRS structural protein, trichohyalin, in *ctsl*$^{-/-}$ HFs. **a:** *ctsl*$^{+/+}$ HFs express intense immunostaining for trichohyalin (red) in the IRS of the lower two-thirds of anagen VI *ctsl*$^{+/+}$ HFs. Note also the presence of trichohyalin in lower medulla of the HF. **b:** Less intense immunostaining for trichohyalin is present in the IRS of anagen VI *ctsl*$^{-/-}$ HFs. IRS, IRS; fp, follicular papilla; Me, medulla. Scale bars, 40 μm (**a** and **b**).

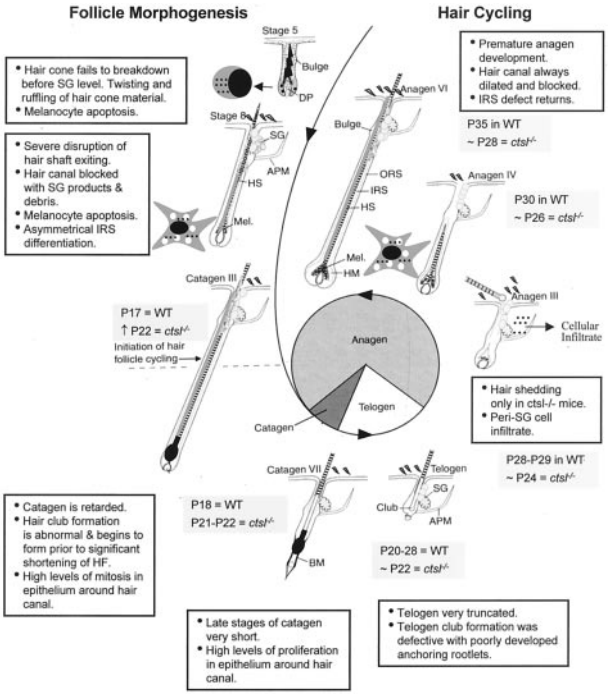

Figure 8. Drawing highlighting abnormalities of HF morphogenesis and hair cycling in *ctsl*$^{-/-}$ mice. **Open boxes** indicate specific defects in structure and in cell kinetics. **Filled boxes** indicate the stage in morphogenesis and cycling representative of most HF at certain days postpartum in *ctsl*$^{+/+}$ and *ctsl*$^{-/-}$ mice. See Results and Discussion for specific descriptions.

shown to be necessary for normal HF development and cycling.[17] Furthermore, unlike many other HF pathology mutants,[2,61] CTSL is also important for homeostasis of the interfollicular epidermis and normal HF pigmentation.[17] This remarkable phenotype of *ctsl*$^{-/-}$ mice seems not to depend on the genetic background in which the mice are maintained. The current analyses were performed with *ctsl*$^{-/-}$ and *ctsl*$^{+/+}$ littermates in a hybrid C57BL/6 × 129 background that originates from the generation of the knockout mice. However, since then the *ctsl*$^{-/-}$ mice were backcrossed for eight generations to obtain congenic mouse lines in the genetic backgrounds C57BL/6, FVB, and 129S2. For those inbred strains the phenotype, ie, the kinetics of hair growth and hair loss, is identical to the mouse strain used in this study (TR and CP, unpublished data). The current study reveals several specific events in HF morphogenesis and cycling during which CTSL plays an important role (Figure 8).

CTSL and HF Morphogenesis

The current study shows that the protease CTSL is involved in the stages of HF morphogenesis associated with keratinization, cornification, and desquamation. These processes are required to form the hair cone, ultimately forming a patent lumen—the hair canal. The breakdown of the hair cone, which caps the emerging hair shaft underneath, is malformed in *ctsl*$^{-/-}$ HFs (Figure 1b) thereby disrupting the release of the hair shaft at the skin surface (Figure 8). This suggests that CTSL is required for the lytic processes involved in hair cone breakdown. It is likely that the substrate for CTSL is present in or close to the hair cone itself, because this program of tissue breakdown is not seen elsewhere in the developing HF at this stage. Hair cone breakdown occurs around the same time as the development of the sebaceous gland duct,[56] which occurs via the breakdown of sebaceous cells. This latter process is also altered in developing *ctsl*$^{-/-}$ HF with resultant misrouting of holocrine sebaceous gland products (Figure 1b, Figure 8)

After hair canal formation, the hair shaft exiting through the hair canal requires continued breakdown of the IRS at the level of the sebaceous gland (Figure 2; a to c).[56] This sequence of degradation events is a prerequisite for the ductal discharge from the sebaceous gland directly into the hair canal to lubricate the emerging hair shaft (Figure 2c). Striking defects were observed in the differentiation/keratinization/desquamation of the IRS proper in the mature stage 8 HF (Figure 2; d to h) indicating that CTSL is important not only for IRS lysis but also for IRS differentiation and cornification/hardening.

We have recently shown that proliferation and apoptosis occur side-by-side during normal HF morphogenesis to ensure proper sculpting of the developing HF.[44] Any imbalance in these stringently coordinated epithelial growth and regression phenomena is likely to result in morphological abnormalities. Therefore, it is noteworthy that *ctsl*$^{-/-}$ mice display an up-regulation of cell proliferation in both the bulbar keratinocyte and melanocyte compartments (Figure 1d and Figure 8). Previously, we reported a three to fourfold increase in Ki67-positive cells in the basal layer of the epidermis in *ctsl*$^{-/-}$ skin.[17] In the present study, a twofold increase in proliferation is detected throughout the entire HF epithelium in *ctsl*$^{-/-}$ mice compared to *ctsl*$^{+/+}$ animals. Although it is not clear whether and how CTSL interacts directly with the proliferation controls of HF cells, the absence of this enzyme may lead to hyperproliferation simply by retarding cell differentiation.

A particularly striking defect in the construction of the pigmentary unit is also a feature of the developing *ctsl*$^{-/-}$ HF. The severe vacuolation that affected many melanocytes at the early stages of melanogenesis (Figure 1d) may be associated with the higher levels of apoptosis in melanogenically active hair bulb melanocytes (Figure 1c and Figure 8). Given the lysosomal origin of melanosomes,[46] these observations suggest that this CTSL activity is involved in the initiation of melanosome organellogenesis and/or melanogenesis. However, the role of CTSL in melanocyte biology seems to be rather subtle, because cytoplasmic vacuolation was restricted only to the early stages in the differentiation of the melanogenically active melanocyte (Figure 1d). Melanogenesis, once started, apparently continues normally in the surviving melanocytes. Moreover, there was no appreciable difference between the pigmentation levels of *ctsl*$^{-/-}$ and *ctsl*$^{+/+}$ hair bulbs when fully developed, suggesting the cells lost through apoptosis are replaced by proliferation, at least for the first hair cycle.

CTSL and HF Cycling

Although *ctsl*$^{-/-}$ mice eventually do develop mature HF (Figure 4b), the absence of CTSL significantly retards the initiation of HF cycling (Figure 4b). In contrast to the abnormally high levels of apoptosis seen during early *ctsl*$^{-/-}$ HF morphogenesis, the retardation of HF regression (catagen) was associated with reduced apoptosis, compared to the massive apoptosis characteristic for *ctsl*$^{+/+}$ HFs.[45] The formation of the normal hair club, an important structure that anchors the hair shaft to the resting telogen HF,[62] only occurs after significant regression of the HF during catagen. However, the lack of CTSL in *ctsl*$^{-/-}$ HFs may result in an extension of the proliferative potential of the HF epithelium and so a delay in terminal differentiation of pre-IRS bulbar keratinocytes. These cells are still identifiable during catagen (Figure 4b). In contrast to the well-formed telogen club-associated anchoring rootlets in *ctsl*$^{+/+}$ HFs, these structures are only poorly formed in *ctsl*$^{-/-}$ HFs (Figure 4h). These structural defects are likely to result in a reduced anchorage of *ctsl*$^{-/-}$ telogen club hairs in the skin and so facilitate their dislodgment at the skin surface, explaining the macroscopic fur phenotype of *ctsl*$^{-/-}$ mice[17] (Figure 4, i and j, and Figure 8). Indeed, murine hair shafts are commonly retained for several hair cycles in murine pelage HF, eg, by mechanisms including strong desmoglein 3-rich attachment plaques[43] and anchoring rootlets.[63] These observations suggest CTSL facilitates tricholemmal keratinization of the epithelial sac surrounding the telogen club.[62]

Structural defects in the *ctsl*$^{-/-}$ club hair, together with the dilation and impaired integrity of the hair canal, are likely to alter interactions between the secondary germ and bulge. These key regions of the telogen HF are recognized sites of stem cells.[64,65] Thus, this process may result in the delivery of signals to the secondary germ cells that are located just under the telogen club and so trigger re-entry into the next hair cycle. In this way, a spontaneous (albeit premature) depilation of *ctsl*$^{-/-}$ hair shafts may trigger a pluck-like response, whereby initiation of cell cycling in the secondary germ occurs before activation of the bulge stem cell compartment.[6,66] The combined effects of defective telogen mooring, a dilated and blocked hair canal, and a peri-sebaceous gland granulocytic infiltrate (Figure 4; i to l, and Figure 8), with potential cytokine release, may activate the closely located secondary germ of the telogen HF to prematurely enter anagen. Thus, the *ctsl*$^{-/-}$ mouse may be a useful model for studying the elusive, yet clinically critical, controls of hair shaft shedding or exogen[3] in which CTSL seems to play a previously unrecognized, functionally important role.

The most striking feature of the *ctsl*$^{-/-}$ HF phenotype is the failure of the anagen-specific IRS to desquamate (Figure 2; d to k). The IRS is thought to serve several crucial functions during normal hair growth. By ensheathing the forming hair shaft, the rigid IRS is thought to mold the malleable hair fiber as it undergoes terminal differentiation/cornification in the proximal HF.[67] This layer also anchors the growing hair shaft within the HF via the imbrication of saw-toothed cuticular cells that line the internal surfaces of the IRS and external surface of the hair shaft.[68] Moreover, the dissolution and shedding of the IRS into the hair canal releases the emerging hair shaft to full function at the skin surface.[3,69,70] The IRS is therefore an excellent marker for orderly HF differentiation and a model for the HF-type epithelial differentiation pathway.[71] It is notable that the IRS is produced only during stages 4 to 8 of HF morphogenesis,[8,53,56] and thereafter repeatedly only during each anagen III to VI phase. The occasional structural defects in the hair shaft itself seen in *ctsl*$^{-/-}$ mice, eg, twisting and even bifurcation (Figure 2k), may result from a disruption of the critical IRS-hair shaft interactions that occur during hardening of the emerging hair shaft. These data suggest that CTSL is required for at least part of the intra- and/or extracellular proteolysis of the differentiating IRS. This lysosomal protease is unlikely however, to be solely responsible for IRS disintegration, given that the *ctsl*$^{-/-}$ IRS looses its cuticular layer before reaching the skin surface (Figure 2; d, g, and h).

A major structural protein found in the IRS is trichohyalin, which functions as a keratin-associated protein supporting the lateral arrangement and aggregation of keratin filaments in IRS cells.[66] In extrafollicular tissues that express trichohyalin, this protein is intimately associated with another keratin-associated protein, filaggrin.[72] Notably, epidermal filaggrin is specifically degraded by CTSL.[73] As previously mentioned, the absence of CTSL also causes epidermal hyperplasia.[17] Thus, it is of interest to note that trichohyalin expression is raised/induced in many cases of epidermal hyperplasia (eg, epidermolytic hyperkeratosis, psoriasis, and so forth).[74] Trichohyalin, a substrate for transglutaminase,[75] is protease-sensitive[76] and so it is likely that CTSL may also use trichohyalin as a protein substrate.

Our findings in *ctsl*$^{-/-}$ mice strongly suggest that the complete IRS terminal differentiation and dissolution is dependent on the CTSL lysosomal proteinase. In the current study, we found a somewhat reduced expression for AE15-positive, granule-bound, epitopes of trichohyalin in *ctsl*$^{-/-}$ HFs compared to *ctsl*$^{+/+}$ HFs. We have also located CTSL protein to the mid-upper ORS in anagen human scalp HFs (DJ Tobin, unpublished data) at a region of the HF where IRS degradation is likely to commence and where AE15-negative granule-free epitopes of trichohyalin occur in more mature IRS cells. Thus, CTSL may play a role in processing the different forms of this structural protein. Further studies are needed to determine whether CTSL degrades this major IRS-cementing protein.

Several studies have suggested a role for the sebaceous gland in the dissolution of the IRS and/or its dissociation from the hair shaft[70,77] including its secretion of relevant lytic enzymes.[2,78] Indeed, the IRS grows out with the hair shaft in the asebia mouse that has hypoplastic sebaceous glands.[79] However, the current study failed to detect significant alterations in sebaceous gland structure apart from the blockage of the sebaceous duct and resultant rerouting of its holocrine-secreted products.

Given that CTSL is a lysosomal protease, it is perhaps not surprising that a deficiency of this enzyme may have implications for lysosome biology, especially the terminal degradation of proteins in the lysosomal compartment of many cells.[80] The striking targeting of differentiating hair bulb melanocytes during the development of the HF pigmentary apparatus in morphogenesis and again during its reconstruction in the cycling HF,[81] suggests that CTSL plays a previously unappreciated role in melanosome biogenesis. The lysosomal origin for this characteristic acidified organelle of pigment cells[46] suggests that melanosomes may become unstable in the absence of CTSL. Interestingly, procathepsin L autocatalytically converts to its mature form at acidic pH.[82] Indeed, recurrent damage to the hair-bulb melanocyte population throughout time may well account for the observed premature canities (graying) in *ctsl*$^{-/-}$ mice. The *ctsl*$^{-/-}$ mouse therefore, provides us with an intriguing model system to assess the role of such proteases in melanosome organellogenesis and/or the initiation of melanogenesis. Interestingly, differentiating hair bulb melanocytes in stage 4 HF, and again in regenerating cycling anagen III/IV *ctsl*$^{-/-}$ HFs, displayed marked melanosome-associated vacuolation (Figure 1d; Figure 2, n and o; Figure 8). Although there was evidence of scattered melanocyte apoptosis during hair development in *ctsl*$^{-/-}$ mice (Figure 1c), significant pigment was produced in young mice (Figure 4b). However, this recurrent defect may ultimately affect the ability of the HF pigmentary unit to regenerate cyclically[81] and may provide useful information on the complex pathogenesis of graying (canities) in the human HF.[82] The vacuolation in *ctsl*$^{-/-}$ hair bulb melanocytes is reminiscent not only of human canities,[83] but more particularly of vitiligo in which it is associated with oxidative stress[84,85] It is possible that the absence of CTSL in the oxygen radical-rich melanosome may reduce their stability, as under normal circumstances the level of this hydrolase is elevated during melanogenesis.[86,87]

In summary, the current study highlights that the lysosomal protease CTSL plays complex, previously unknown, roles in epidermal, pigment, and HF biology (Figure 8). As shown here, the involvement of CTSL in HF biology occurs most predominantly in the differentiation and proteolysis of the IRS but also in the proliferation, apoptosis, and differentiation of cortical and IRS keratinocytes, and melanogenically active hair-bulb melanocytes. Given the striking IRS phenotype in this knockout, a structural protein (perhaps trichohyalin) is a likely HF substrate for this protease. This model permits the dissection of several important events in HF development, cycling, and hair shaft shedding and confirms the important roles of protease-anti-protease systems in cutaneous biology.

Acknowledgments

We thank Dr. W. Roth for her important role in initiating this study; and S. Dollwet, G. Pilnitz-Stolze, and S. Wegerich for their technical support.

References

1. Paus R, Cotsarelis G: The biology of hair follicles. N Engl J Med 1999, 341:491–497
2. Cotsarelis G, Millar SE: Towards a molecular understanding of hair loss and its treatment. Trends Mol Med 2001, 7: 293–301
3. Stenn KS, Paus R: Controls of hair follicle cycling. Physiol Rev 2001, 81:449–494
4. Schaller SA, Li S, Ngo-Muller V, Han MJ, Omi M, Anderson R, Muneoka K: Cell biology of limb patterning. Int Rev Cytol 2001, 203:483–517
5. Chuong C-M: Molecular Basis of Epithelial Appendage Morphogenesis. Edited by C-M Chuong. Austin, R.G. Landes Company, 1998
6. Hardy MH: The secret life of the hair follicle. Trends Genet 1992, 8:55–61
7. Philpott MJ, Paus R: Principles of hair follicle morphogenesis. Molecular Basis of Epithelial Appendage Morphogenesis. Edited by C-M Chuong. Austin, R.G. Landes Company, 1998, pp 75–103
8. Paus R, Müller-Röver S, Botchkarev VA: Chronobiology of the hair follicle: hunting the "hair cycle clock." J Invest Dermatol Symp Proc 1999, 4:338–345
9. Kawabe TT, Rea TJ, Flenniken AM, Williams BR, Groppi VE, Buhl AE: Localization of TIMP in cycling mouse hair. Development 1991, 111: 877–879
10. Krejci-Papa NC, Paus R: A novel in-situ-zymography technique localizes gelatinolytic activity in human skin to mast cells. Exp Dermatol 1998, 7:321–326
11. Yamazaki M, Tsuboi R, Lee YR, Ishidoh K, Mitsui S, Ogawa H: Hair cycle-dependent expression of hepatocyte growth factor (HGF) activator, other proteinases, and proteinase inhibitors correlates with the expression of HGF in rat hair follicles. J Invest Dermatol Symp Proc 1999, 4:312–315
12. Lee YR, Yamazaki M, Mitsui S, Tsuboi R, Ogawa H: Hepatocyte growth factor (HGF) activator expressed in hair follicles is involved in in vitro HGF-dependent hair follicle elongation. J Dermatol Sci 2001, 25:156–163
13. Karelina TV, Bannikov GA, Eisen AZ: Basement membrane zone remodeling during appendageal development in human fetal skin. The absence of type VII collagen is associated with gelatinase-A (MMP2) activity. J Invest Dermatol 2000, 114:371–375
14. Sonoda T, Asada Y, Kurata S, Takayasu S: The mRNA for protease nexin-1 is expressed in human dermal papilla cells and its level is affected by androgen. J Invest Dermatol 1999, 113:308–313
15. Ekholm E, Egelrud T: The expression of stratum corneum chymotryptic enzyme in human anagen hair follicles: further evidence for its involvement in desquamation-like processes. Br J Dermatol 1998, 139:585–590
16. Nakagawa T, Roth W, Wong P, Nelson A, Farr A, Deussing J, Villadangos JA, Ploegh H, Peters C, Rudensky AY: Cathepsin L: critical role in Ii degradation and CD4 T cell selection in the thymus. Science 1998, 280:450–453
17. Roth W, Deussing J, Botchkarev VA, Pauly-Evers M, Saftig P, Hafner A, Schmidt P, Schmahl W, Scherer J, Anton-Lamprecht I, Von Figura K, Paus R, Peters C: Cathepsin L deficiency as molecular defect of furless: hyperproliferation of keratinocytes and perturbation of hair follicle cycling. FASEB J 2000, 14:2075–2086
18. Turk B, Turk D, Turk V: Lysosomal cysteine proteases: more than scavengers. Biochim Biophys Acta 2000, 7:98–111
19. Afonso S, Romagnano L, Babiarz B: Expression of cathepsin proteinases by mouse trophoblast in vivo and in vitro. Dev Dyn 1999, 216:374–384
20. Afonso S, Romagnano L, Babiarz B: The expression and function of cystatin C and cathepsin B and cathepsin L during mouse embryo implantation and placentation. Development 1997, 124:3415–3425
21. Dohchin A, Suzuki JI, Seki H, Masutani M, Shiroto H, Kawakami Y: Immunostained cathepsins B and L correlate with depth of invasion and different metastatic pathways in early stage gastric carcinoma. Cancer 2000, 89:482–487
22. Iwata Y, Mort JS, Tateishi H, Lee ER: Macrophage cathepsin L, a factor in the erosion of subchondral bone in rheumatoid arthritis. Arthritis Rheum 1997, 40:499–509
23. Morris VL, Tuck AB, Wilson SM, Percy D, Chambers AF: Tumor progression and metastasis in murine D2 hyperplastic alveolar nodule mammary tumor cell lines. Clin Exp Metastasis 1993, 11:103–112

24. Ohba T, Ohba Y, Moriyama K: Synthesis of mRNAs for cathepsins L and K during development of the rat mandibular condylar cartilage. Cell Tissue Res 2000, 302:343–352
25. Felbor U, Dreier L, Bryant RA, Ploegh HL, Olsen BR, Mothes W: Secreted cathepsin L generates endostatin from collagen XVIII. EMBO J 2000, 19:1187–1194
26. Thewes M, Engst R, Jurgens M, Borelli S: Immunohistochemical analysis of procathepsin L and cathepsin B in cutaneous Kaposi's sarcoma. Int J Dermatol 1997, 36:100–103
27. Ishidoh K, Kominami E: Gene regulation and extracellular functions of procathepsin L. Biol Chem 1998, 379:131–135
28. Lemaire R, Huet G, Zerimech F, Grard G, Fontaine C, Duquesnoy B, Flipo: RM selective induction of the secretion of cathepsins B and L by cytokines in synovial fibroblast-like cells. Br J Rheumatol 1997, 36:735–743
29. Janulis M, Silberman S, Ambegaokar A, Gutkind JS, Schultz RM: Role of mitogen-activated protein kinases and c-Jun/AP-1 trans-activating activity in the regulation of protease mRNAs and the malignant phenotype in NIH 3T3 fibroblasts. J Biol Chem 1999, 274:801–813
30. Gerber A, Wille A, Welte T, Ansorge S, Buhling F: Interleukin-6 and transforming growth factor-beta 1 control expression of cathepsins B and L in human lung epithelial cells. J Interferon Cytokine Res 2001, 21:11–19
31. Turksen K, Kupper T, Degenstein L, Williams I, Fuchs E: Interleukin 6: insights to its function in skin by overexpression in transgenic mice. Proc Natl Acad Sci USA 1992, 89:5068–5072
32. Foitzik K, Lindner G, Mueller-Roever S, Maurer M, Botchkareva N, Botchkarev V, Handjiski B, Metz M, Hibino T, Soma T, Dotto GP, Paus R: Control of murine hair follicle regression (catagen) by TGF-beta1 in vivo. FASEB J 2000, 14:752–760
33. Liuzzo JP, Petanceska SS, Devi LA: Neurotrophic factors regulate cathepsin S in macrophages and microglia: a role in the degradation of myelin basic protein and amyloid beta peptide. Mol Med 1999, 5:334–343
34. du Cros DL: Fibroblast growth factor influences the development and cycling of murine hair follicles. Dev Biol 1993, 156:444–453
35. Botchkareva NV, Botchkarev VA, Albers KM, Metz M, Paus R: Distinct roles for nerve growth factor and brain-derived neurotrophic factor in controlling the rate of hair follicle morphogenesis. J Invest Dermatol 2000, 114:314–320
36. Damiens C, Grimaud E, Rousselle AV, Charrier C, Fortun Y, Heymann D, Padrines M: Cysteine protease production by human osteosarcoma cells (MG63, SAOS2) and its modulation by soluble factors. Cytokine 2000, 12:539–542
37. Stenn KS, Parimoo S, Prouty S: Growth of the hair follicle: a cycling and regenerating biological system. Molecular Basis of Epithelial Appendage Morphogenesis. Edited by C-M Chuong. Austin, R. G. Landes, 1999, pp 229–236
38. Kim K, Cai J, Shuja S, Kuo T, Murnane MJ: Presence of activated ras correlates with increased cysteine proteinase activities in human colorectal carcinomas. Int J Cancer 1998, 79:324–333
39. Pierce AM, Fisher SM, Conti CJ, Johnson DG: Deregulated expression of E2F1 induces hyperplasia and cooperates with ras in skin tumor development. Oncogene 1998, 16:1267–1276
40. Ferreras M, Felbor U, Lenhard T, Olsen BR, Delaisse J: Generation and degradation of human endostatin proteins by various proteinases. FEBS Lett 2000, 486:247–251
41. Mecklenburg L, Tobin DJ, Müller-Röver S, Handjiski B, Wendt G, Peters EM, Pohl S, Moll I, Paus R: Active hair growth (anagen) is associated with angiogenesis. J Invest Dermatol 2000, 114:909–916
42. Mecklenburg L, Tobin DJ, Paus R: Hair follicle involution (catagen) is accompanied by apoptosis-driven regression of cutaneous microvasculature. J Invest Dermatol 2000, 117:427A
43. Koch PJ, Mahoney MG, Cotsarelis G, Rothenberger K, Lavker RM, Stanley JR: Desmoglein 3 anchors telogen hair in the follicle. J Cell Sci 1998, 111:2529–2537
44. Magerl M, Tobin DJ, Müller-Röver S, Hagen E, Lindner G, McKay IA, Paus R: Patterns of proliferation and apoptosis during murine hair follicle morphogenesis. J Invest Dermatol 2001, 116:947–955
45. Lindner G, Botchkarev VA, Botchkareva NV, Ling G, van der Veen C, Paus R: Analysis of apoptosis during hair follicle regression (catagen). Am J Pathol 1997, 151:1601–1617
46. Orlow SJ: Melanosomes are specialized members of the lysosomal lineage of organelles. J Invest Dermatol 1995, 105:3–7
47. Müller-Röver S, Handjiski B, van der Veen C, Eichmuller S, Foitzik K, McKay IA, Stenn KS, Paus R: A comprehensive guide for the accurate classification of murine hair follicles in distinct hair cycle stages. J Invest Dermatol 2001, 117:3–15
48. Karnovsky MJ: A formaldehyde-glutaraldehyde fixative of high osmolarity for use in electron microscopy. J Cell Biol 1965, 27:137a–138a
49. Tobin DJ, Fenton DA, Kendall MD: Ultrastructural observations on the hair bulb melanocytes and melanosomes in acute alopecia areata. J Invest Dermatol 1990, 94:803–807
50. Tobin DJ, Hagen E, Botchkarev VA, Paus R: Do hair bulb melanocytes undergo apoptosis during hair follicle regression (catagen)? J Invest Dermatol 1998, 111:941–947
51. Young RD: Morphological and ultrastructural aspects of the dermal papilla during the growth cycle of the vibrissal follicle in the rat. J Anat 1980, 131:355–365
52. Bulfone-Paus S, Ungureanu D, Pohl T, Lindner G, Paus R, Ruckert R, Krause H, Kunzendorf U: Interleukin-15 protects from lethal apoptosis in vivo. Nat Med 1997, 3:1124–1128
53. Pinkus H: Embryology of hair. The Biology of Hair Growth. Edited by W Montagna, RA Ellis. New York, Academic Press, 1958, pp 1–32
54. Paus R, Müller-Röver S, Van Der Veen C, Maurer M, Eichmuller S, Ling G, Hofmann U, Foitzik K, Mecklenburg L, Handjiski B: A comprehensive guide for the recognition and classification of distinct stages of hair follicle morphogenesis. J Invest Dermatol 1999, 113: 523–532
55. Müller-Röver S, Handjiski B, Van der Ween C, Eichmuller S, Foitzik K, McKay I, Stenn KS, Paus R: A comprehensive guide for the accurate classification of murine hair follicles in distinct hair cycle stages. J Invest Dermatol 2001, 117:3–15
56. Robins EJ, Breathnach AS: Fine structure of the human fetal hair follicle at hair-peg and early bulbous-peg stages of development. J Anat 1969, 104:553–569
57. Bell M: Ultrastructure of differentiating hair follicles. Advances in Biology of Skin, Hair Growth, vol. 9. Edited by W Montagna, RL Dobson. Oxford, Pergamon Press, 1967, pp 61–81
58. Slominski A, Paus R, Costantino R: Differential expression and activity of melanogenesis-related proteins during induced hair growth in mice. J Invest Dermatol 1991, 96:172–179
59. Slominski A, Paus R: Melanogenesis is coupled to murine anagen: toward new concepts for the role of melanocytes and the regulation of melanogenesis in hair growth. J Invest Dermatol 1993, 101:90S–97S
60. Reynolds J: The epidermal melanocytes of mice. J Anat 1954, 88: 45–58
61. Nakamura M, Sundberg JP, Paus R: Mutant laboratory mice with abnormalities in hair follicle morphogenesis, cycling, and/or structure: annotated tables. Exp Dermatol 2001, 10:369–390
62. Pinkus H, Iwasaki T, Mishima Y: Outer root sheath keratinization in anagen and catagen of the mammalian hair follicle. A seventh distinct type of keratinization in the hair follicle: trichilemmal keratinization. J Anat 1981, 133:19–35
63. Chase HB, Eaton GJ: The growth of hair follicles in waves. Ann NY Acad Sci 1959, 83:365–368
64. Cotsarelis G, Sun TT, Lavker RM: Label retaining cells reside in the bulge area pilosebaceous unit: implications for follicular stem cells, hair cycle, and skin carcinogenesis. Cell 1990, 61:1329–1337
65. Panteleyev AA, Jahoda CAB, Christiano AM: Hair follicle predetermination. J Cell Sci 2001, 114:3419–3431
66. O'Guin WM, Sun TT, Manabe M: Interaction of trichohyalin with intermediate filaments: three immunologically defined stages of trichohyalin maturation. J Invest Dermatol 1992, 98:24–32
67. Forslind B: Structure and function of hair follicle. Hair and Its Disorders. Edited by FM Camacho, VA Randall, VH Price. London, Martin Dunitz, 2000, pp 3–17
68. Birbeck MSC, Mercer EH: The electron microscopy of the human hair follicle. Part 2: the hair cuticles. J Biophys Biochem Cytol 1957, 3:215–221
69. Straile WE: Possible functions of the external root sheath during the growth of the hair follicle. J Exp Zool 1962, 150:207–224
70. Gemmell RT, Chapman RE: Formation and breakdown of the inner root sheath and features of the pilary canal epithelium in the wool follicle. J Ultrastruct Res 1971, 36:355–366
71. Powell BC, Rogers GE: The role of keratin proteins and their genes in the growth, structure and properties of hair. Formation and Structure

of Human Hair. Edited by P Jolles, H Zahn, H Höcker. Basel, Birkhauser Verlag, 1997, pp 59–148
72. Manabe M, O'Guin WM: Existence of trichohyalin-keratohyalin hybrid granules: co-localization of two major intermediate filament-associated proteins in non-follicular epithelia. Differentiation 1994, 58:65–75
73. Kawada A, Hara K, Kominami E, Tezuka T, Takahashi M, Takahara H: Precursor of rat epidermal cathepsin L: purification and immunohistochemical localization. J Dermatol Sci 2000, 23:36–45
74. O'Guin WM, Manabe M: The role of trichohyalin in hair follicle differentiation and its expression in nonfollicular epithelia. The molecular and structural biology of hair. Ann NY Acad Sci 1991, 642:51–63
75. Harding HW, Rogers GE: Epsilon-(gamma-glutamyl)lysine cross-linkage in citrulline-containing protein fractions from hair. Biochemistry 1971, 10:624–630
76. Rothnagel JA, Rogers GE: Trichohyalin, an intermediate filament-associated protein of the hair follicle. J Cell Biol 1986, 102:1419–1429
77. Puccinelli VA, Caputo R, Ceccarelli B: The structure of human hair follicle and hair shaft: an electron microscope study. G Ital Dermatol Minerva Dermatol 1967, 108:453–497
78. Williams D, Stenn KS: Transection level dictates the pattern of hair follicle sheath growth in vitro. Dev Biol 1994, 165:469–479
79. Sundberg JP, Boggess D, Sundberg BA, Eilertsen K, Parimoo S, Filippi M, Stenn K: Asebia-2J (Scd1(ab2J)): a new allele and a model for scarring alopecia. Am J Pathol 2000, 156:2067–2075
80. Barrett AJ, Kirschke H: Cathepsin B, cathepsin H, and cathepsin L. Methods Enzymol 1981, 80:535–561
81. Tobin DJ, Slominski A, Botchkarev V, Paus R: The fate of hair follicle melanocytes during the hair growth cycle. J Invest Dermatol Symp Proc 1999, 4:323–332
82. Ishidoh K, Kominami E: Multi-steps in the processing of procathepsin L in vitro. FEBS Lett 1994, 352:1281–1284
83. Tobin DJ, Paus R: Graying: gerontobiology of the hair follicle pigmentary unit. Exp Gerontol 2001, 36:29–54
84. Westerhof W, Njoo D, Menke KE: Miscellaneous hypomelanoses: disorders characterized by extra-cutaneous loss of pigmentation. The Pigmentary System: Physiology and Pathophysiology. Edited by JJ Nordlund, RE Boissy, VJ Hearing, RA King, J-P Ortonne. New York, Oxford University Press, 1998, pp 475–487
85. Tobin DJ, Swanson NN, Pittelkow MR, Peters EM, Schallreuter KU: Melanocytes are not absent in lesional skin of long duration vitiligo. J Pathol 2000, 191:407–416
86. Diment S, Eidelman M, Rodriguez GM, Orlow SJ: Lysosomal hydrolases are present in melanosomes and are elevated in melanizing cells. J Biol Chem 1995, 270:4213–4215
87. Botchkareva NV, Khlgatian M, Longley BJ, Botchkarev VA, Gilchrest BA: SCF/c-kit signaling is required for cyclic regeneration of the hair pigmentation unit. FASEB J 2001, 15:645–658